

## Supporting information

### **The thermal stability of carbonaceous materials is too low for applications in direct NO decomposition catalysis**

*Maurice Vennewald* ♦, *Daniel Ditz* ♦, *Andree Iemhoff* ♦, *Regina Palkovits* ♦\*

♦ Chair of Heterogeneous Catalysis and Chemical Technology, ITMC, RWTH Aachen University, Worringerweg 2, DE-52074 Aachen, Germany. E-mail: [palkovits@itmc.rwth-aachen.de](mailto:palkovits@itmc.rwth-aachen.de)

#### **Corresponding Author**

\* Regina Palkovits: [palkovits@itmc.rwth-aachen.de](mailto:palkovits@itmc.rwth-aachen.de)

## Materials

### *CW20-activated carbon*

CW20 activated coal was purchased from Silcarbon and used as received.

### *g-CN*

g-CN was synthesized according to the procedure reported by Zhu *et al.*. Cyanamide (4.5 g) was treated in static air by increasing the temperature from ambient to 550 °C at 2 °C min<sup>-1</sup> and holding for 4 h. A yellow powder was obtained.

### *Zn-g-CN*

Zn-g-CN was synthesized according to the procedure reported by Zhu *et al.*. Cyanamide (4.5 g) was dissolved in demineralized water (25 mL) under stirring. After adding ZnCl solution (1 mL, 0.0152 M) the solution was heated to 90 °C until all water was evaporated. The resulting powder was dried at 110 °C over night and treated in static air by increasing the temperature from ambient to 550 °C at 2 °C min<sup>-1</sup> and holding for 4 h. A yellow powder was obtained.

### *Cu- and Fe-g-CN*

Cu- and Fe-g-CN were synthesized by stirring g-CN (400 mg) with Cu(OAc)<sub>2</sub> (11.4 mg) or FeNO<sub>3</sub> · 9H<sub>2</sub>O (28.8 mg) in demineralized water (250 mL) for 24 h. Targeting 1 wt% metal loading. The dispersion was filtrated and the resulting powder dried at 110 °C for 24 h.

### *CTF-Py*

All reagents were stored and processed in a glovebox. 1,6-dicyanopyridine (3 g, 1 eq.) and zinc chloride (18.8 g, 5 eq., Redi-Dri™, Sigma Aldrich, >98%) were transferred into a mortar, mixed and ground well. The mixture was transferred into a quartz glass ampoule. The ampoule was equipped with a valve to retain inert atmosphere when taking it from the glovebox. After evacuation for at least 4 hours at <0.02 mbar the ampoule was sealed. In a muffle furnace, the temperature was programmed to be held 10 h at 400 °C and 10 h at 600 °C with a heating rate of 10 °C min<sup>-1</sup> for each transition. After cooling to room temperature, the glass was broken

carefully and the resulting monolith was soaked in HCl (1 M) and washed with water (300 mL). The black powder was dried at 80 °C, ground in a ball mill (Fritsch Pulverisette, 5 min, 30 Hz) and refluxed in aq. HCl solution (400 mL, 6 M) overnight. Afterwards in a sequence of washing steps, the powder was stirred in aq. NaOH solution (400 mL, 6 M) at 60 °C overnight, refluxed in water at 100 °C overnight and stirred in THF at 60 °C for 6 hours. After drying at 60 °C in vacuum, a black powder was obtained.

## **Material characterization**

### *Nitrogen Physisorption*

Nitrogen physisorption experiments were conducted with a Quadrasorb SI instrument at 77 K. Before each measurement, adsorbates were removed under vacuum at 150 °C for at least 5 h. The software QuadraWin was used for data evaluation and the BET model was used to obtain the specific surface area (range  $0.05 \leq p/p_0 \leq 0.2$ ). The total pore volume was obtained for the volume adsorbed at the relative pressure  $p/p_0 = 0.95$ .

### *Elemental analysis*

Elemental composition of the support materials was determined with an Elementar Vario EL cube by combustion analysis.

### *Thermogravimetric analysis*

Thermogravimetric analysis was conducted using a Netzsch STA 409 by heating from ambient to 1000 °C with 10 °C min<sup>-1</sup> in flowing air.

### *X-ray diffraction*

XRD was performed using a Bruker second generation D2 phaser equipped with a Cu K<sub>α</sub> source and a XE-T detector scanning from 6 to 90° with 0.02° and 0.4s per step.

### *Mott-Schottky measurements*

All electrochemical measurements were performed with a three electrode set-up, using a Pt counter electrode, a Ag/AgCl (3 M NaCl) reference electrode and NaSO<sub>4</sub> (2 M in water) as

electrolyte. The working electrode was fabricated by mixing 5 mg material (particle size <40  $\mu\text{m}$ ) with water, ethanol (50  $\mu\text{L}$  each) and 1 wt% Nafion solution for 30 mins under sonication. Then, 2  $\mu\text{L}$  of the suspension was dropcasted onto 0.25  $\text{cm}^2$  of a FTO substrate and dried under ambient conditions. Spare FTO surface was covered with an isolating paint. The sample was conditioned via 30 CV cycles between -0.2 V and 1.2 V (100  $\text{mV s}^{-1}$ ). MS analysis is conducted at  $\text{pH} = 7$  between -0.1 V and 1.2 V in 0.05 V steps at different frequencies.

### *UV-VIS measurements*

UV-VIS diffuse reflectance spectroscopy of the undiluted samples was performed on a Lambda 7 device from Perkin-Elmer with the respective accessory. The spectra were recorded in a range of 300-700 nm with a resolution of 1 nm against  $\text{BaSO}_4$  as standard. The device changed the light source from a halogen lamp to a deuterium lamp for wavelengths smaller 319 nm. The PerkinElmer UV-Winlab 2.80.03 software package was used for measurement control and data analysis. The band gap was determined via the Tauc-plot method.

### *Metal loading*

The determination of Zn, Fe and Cu amounts in the respective g-CNs was conducted by Mikrolab Kolbe, Oberhausen.

### **Reaction measurements**

Gases (99,999% purity) were obtained from Westfalen (1%  $\text{NO}/\text{Ar}$ ; 5%  $\text{O}_2/\text{Ar}$ ; He; Ar). Gas flows were controlled by mass flow controllers (Bronkhorst/MKS Instruments). Concentrations of  $\text{N}_2$  (amu 28),  $\text{O}_2$  (amu 32),  $\text{NO}$  (amu 30),  $\text{N}_2\text{O}$  (amu 44) were measured using a Cirrus 2 mass spectrometer (MKS Instruments) with He as an internal reference. The outlet stream was further analyzed employing a Spectrum 2 IR spectrometer (Perkin Elmer) equipped with a 2.4 m long-path gas cell (Pike technologies) heated to 120  $^\circ\text{C}$ .

Samples were held on a porous quartz disk (4.2 mm) covered with 1 mm quartz wool within a U-shaped quartz reactor.

For direct  $\text{NO}$  decomposition experiments samples were heated to 350  $^\circ\text{C}$  at 10  $^\circ\text{C min}^{-1}$  in flowing 10%  $\text{He}/\text{Ar}$  (50  $\text{mL min}^{-1}$ ) and hold for 1 h prior to reaction. Then the gas stream was

switched to bypass and set to 0.5% NO/10% He/Ar ( $100 \text{ mL/min}^{-1}$ ; GHSV =  $30000 \text{ h}^{-1}$ ). After stabilization, the stream was switched to reactor. Temperature was increased in  $50 \text{ }^\circ\text{C}$  steps ( $10 \text{ }^\circ\text{C/min}$ ) to  $550 \text{ }^\circ\text{C}$  with at least 10 min measuring time after temperature equilibration. Conversion and yields were calculated as a difference between bypass concentration and reactor concentration at the respective temperatures.

For temperature programmed oxidation (TPO) experiments, samples were heated from ambient to  $600 \text{ }^\circ\text{C}$  with  $10 \text{ }^\circ\text{C min}^{-1}$  in 0.5%  $\text{O}_2/10\%$  He/Ar ( $50 \text{ mL/min}^{-1}$ ; GHSV =  $30000 \text{ h}^{-1}$ ).

## XRD

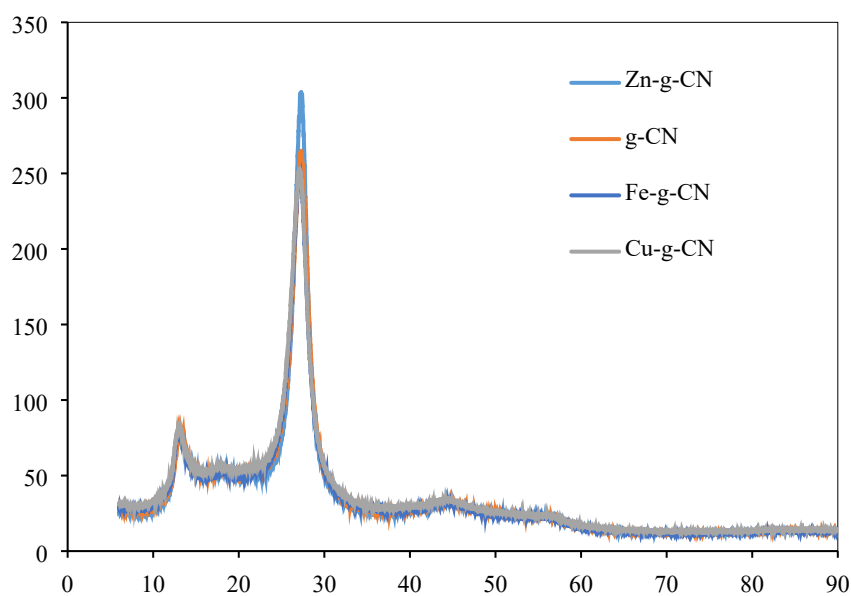


Fig. S 1: X-ray diffractogram of g-CN, Zn-g-CN, Fe-g-CN and Cu-g-CN.

## Mott-Schottky Plots

g-CN

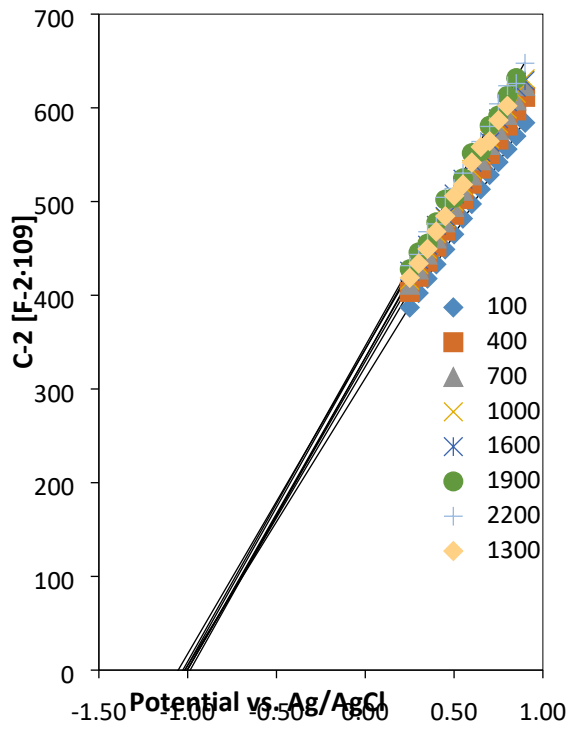


Fig. S 2: Mott-Schottky Plot of g-CN at (sample 1).

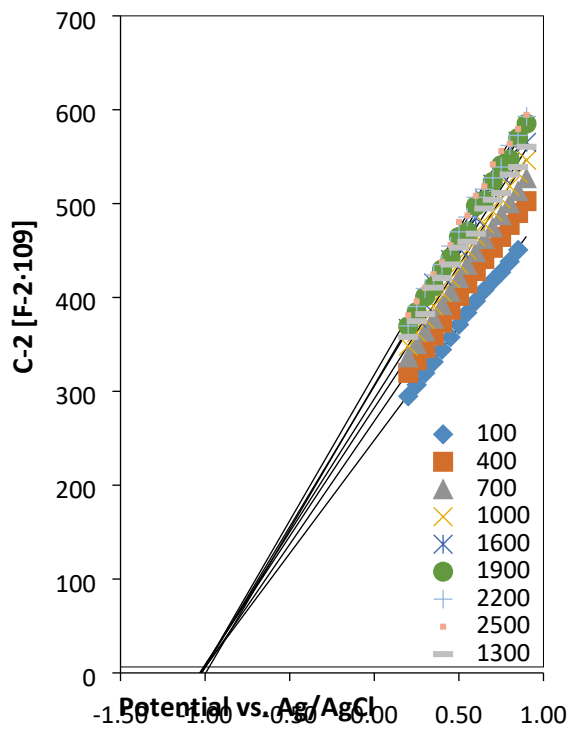


Fig. S 3: Mott-Schottky Plot of g-CN (sample 2).

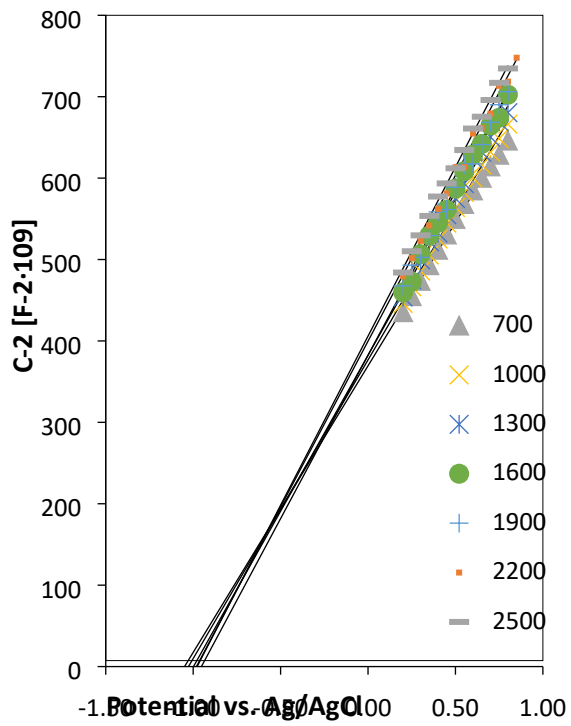


Fig. S 4: Mott-Schottky Plot of g-CN (sample 3).

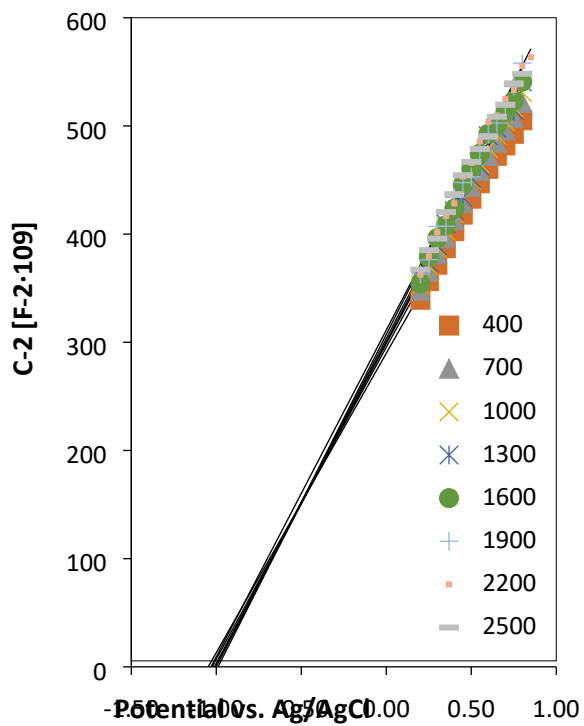


Fig. S 5: Mott-Schottky Plot of Zn-g-CN (sample 1).

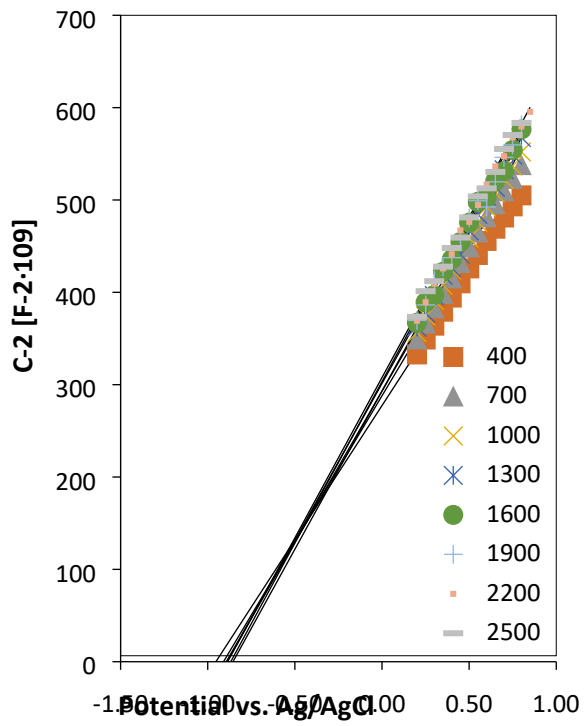


Fig. S 6: Mott-Schottky Plot of Zn-g-CN (sample 2).

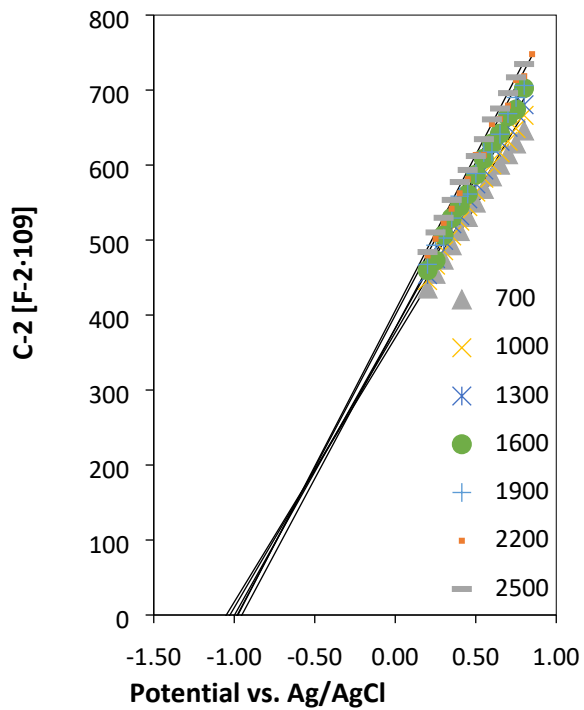


Fig. S 7: Mott-Schottky Plot of Zn-g-CN (sample 3).



## UV-VIS

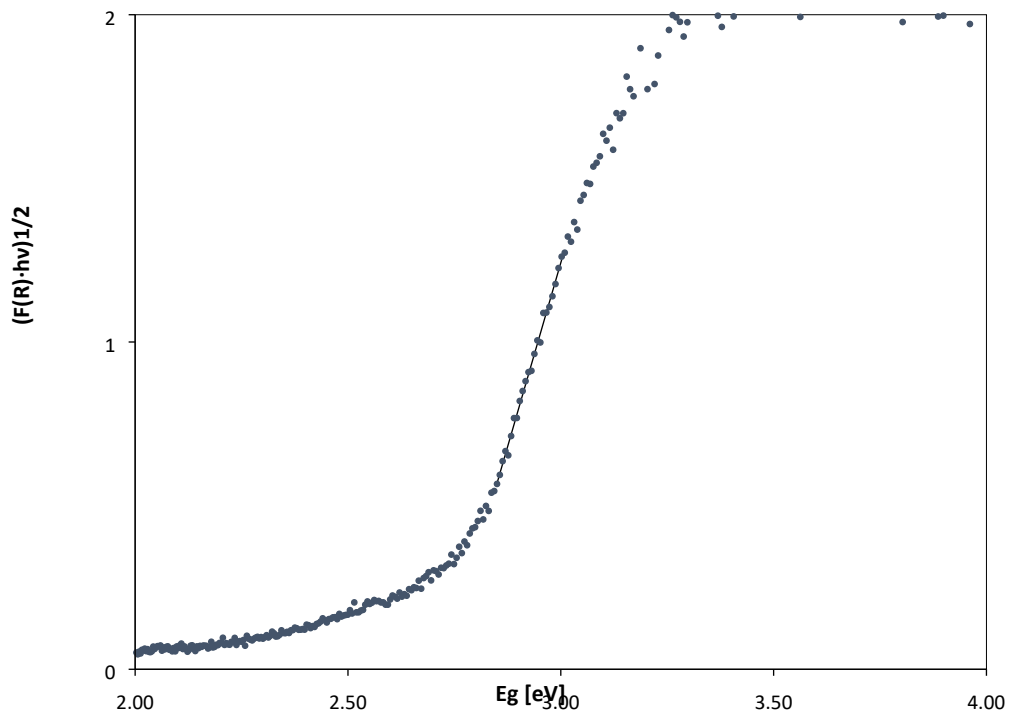


Fig. S 8: Tauc plot with linear regression formula for g-CN.

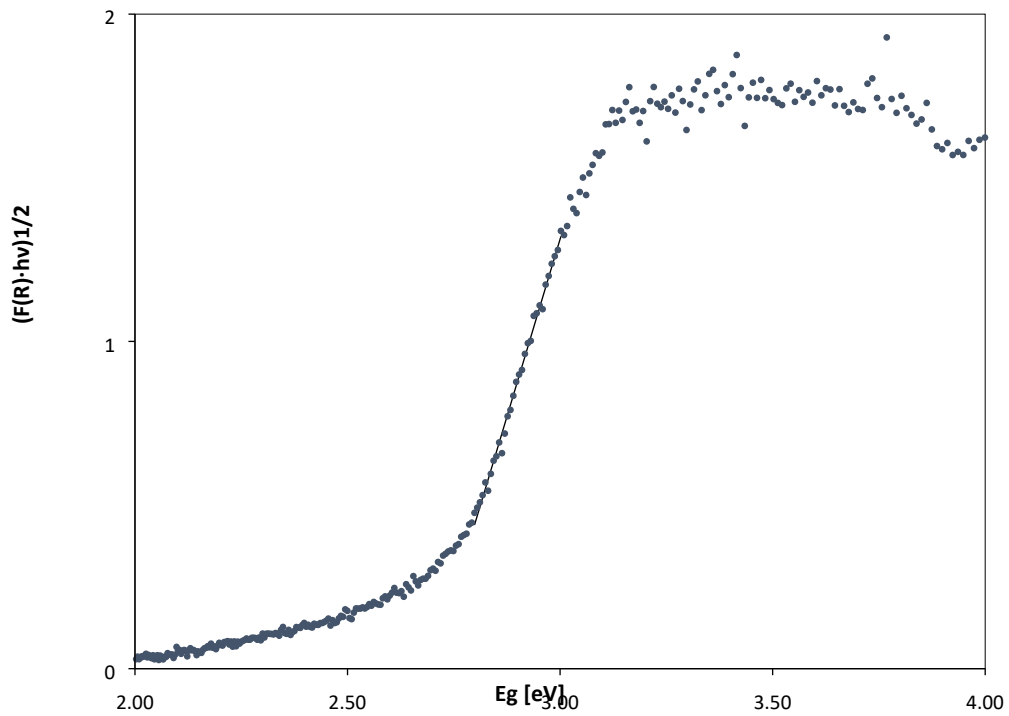


Fig. S 9: Tauc plot with linear regression formula for Zn-g-CN.

## N<sub>2</sub>-Physiosorption

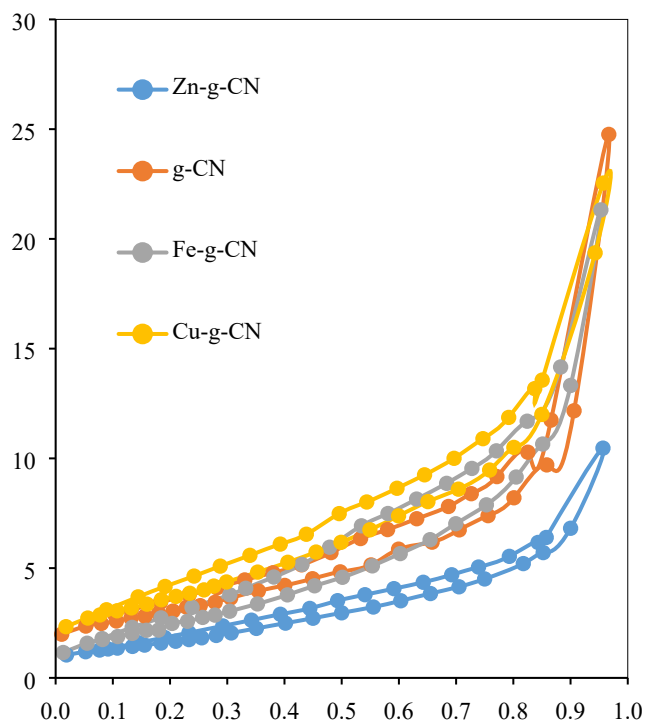


Fig. S 10: Isotherms of g-CN and metal doped g-CNs.

Tab S 1: BET surface areas of employed materials.

Material	BET surface area (m <sup>2</sup> g <sup>-1</sup> )
g-CN	11
Cu-g-CN	13
Fe-g-CN	9
Zn-g-CN	6
CTF	860
CW-20	2023

## CHN

Table S 2: CHN amounts of g-CN materials prior to and after reaction (used).

Material	C (%)	H (%)	N (%)
g-CN	34.4	1.8	62.7
g-CN-used	24.3	2.0	42.2
Zn-g-CN	33.8	1.9	62.0
Zn-g-CN-used	35.0	1.6	62.0
theoretical	39.1	0	60.9

## MS Analytics of exhaust stream

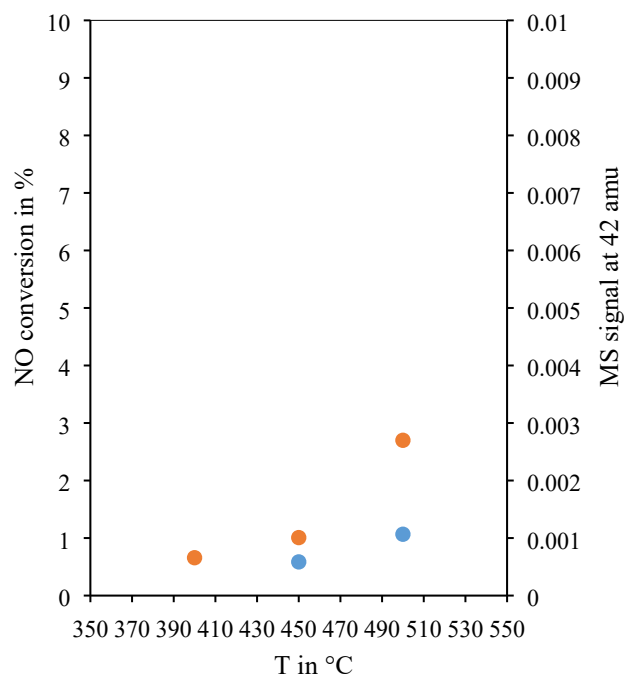


Fig. S 11: Comparison of NO conversion for g-CN (blue) with mass spectrometry signal at 43 amu (orange).

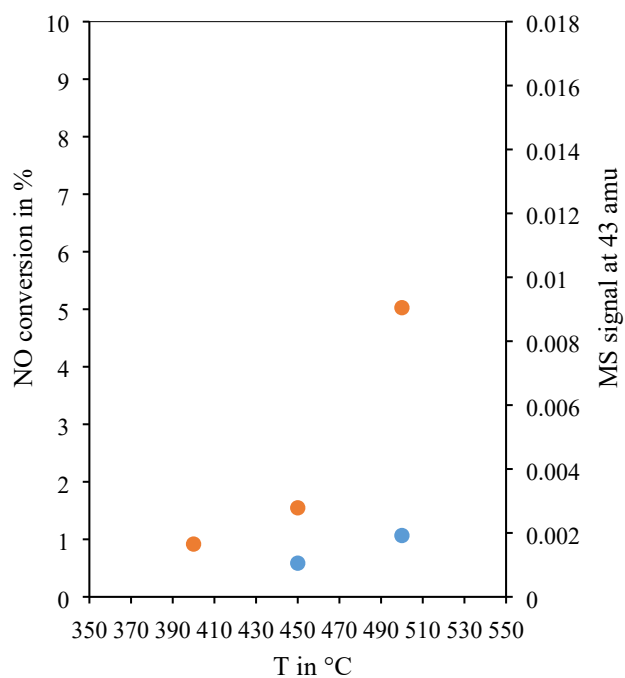


Fig. S 12 Comparison of NO conversion for g-CN (blue) with mass spectrometry signal at 43 amu (orange).

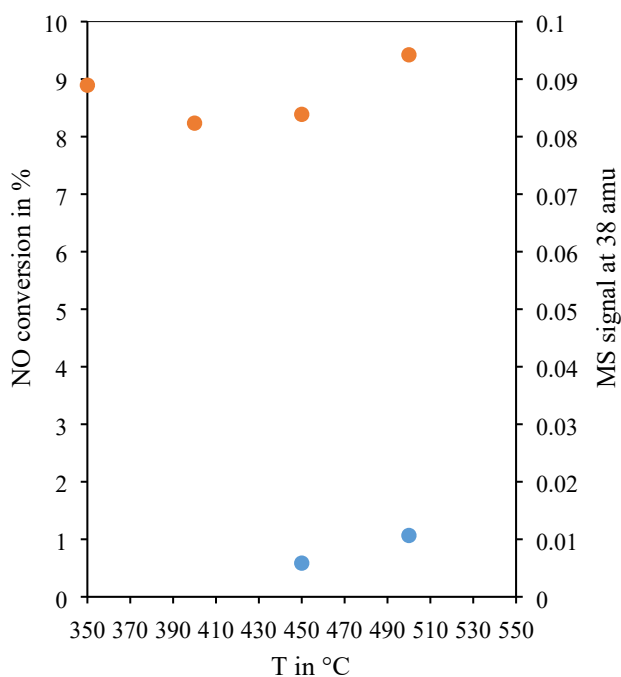


Fig. S 13: Comparison of mass spectrometry signal at 38 amu (orange) with NO conversion (blue) for g-CN. In contrast to 42 and 43 amu no correlation is observable, excluding the possibility that these correlations are data artefacts.

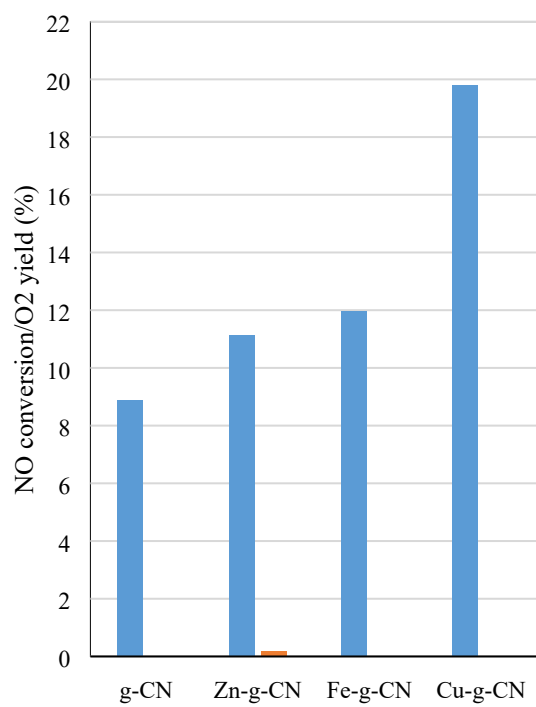


Fig. S 14: NO conversion (blue) and O<sub>2</sub> yield (orange) for g-CN, Zn-g-CN, Fe-g-CN and Cu-g-CN. Showing no detectable O<sub>2</sub> yield for all samples.